



A Recycled-Material-Based Electrochemical Eco-sensor for Sensitive Detection of Antischistosomal Drug Residues in Bovine-Derived Food Samples

Khalid A. M. Attia¹ · Ahmed E. F. Abbas² · Ahmed El-Olemy¹ · Nahla A. Abdelshafi³ · Sherif M. Eid²

Received: 27 November 2023 / Revised: 16 January 2024 / Accepted: 28 January 2024
© The Author(s) 2024

Abstract

Veterinary drug residues in food have emerged as an urgent threat to consumer safety. Herein, we present the first square wave voltammetric method for the trace-level detection of cinnarizine residues, a recently used antischistosomal drug, in bovine food samples. The method depends on the electrochemical oxidation after modification of the carbon paste sensor with recycled Al_2O_3 -NPs functionalized multi-walled carbon nanoparticles. The produced sensor (Al_2O_3 -NPs/MWCNTs/CPE) was characterized using the transmission electron microscope, scanning electron microscope, Fourier-transform infrared spectroscopy, energy-dispersive spectrometer, and X-ray diffractometer that confirm the successful incorporation of the Al_2O_3 -NPs/MWCNTs composite into the modified electrode. As expected, the active surface area and electron transfer processes were accelerated by the modification, which was evidenced by cyclic voltammetry, chronoamperometric studies, scan rate studies, and electrochemical impedance spectroscopy. Compared to previous techniques, this facile sensor demonstrated enhancements across critical analytical criteria including the detection limit of 0.17 nM, linear response across 5–100 nM ($r^2 = 0.998$), accuracy ranging from 96.5 to 103.2%, precision below 0.81% relative standard deviation, reproducibility within 0.36% range, 20 s response time and applicability in spiked food matrices. In addition, five different greenness and whiteness tools quantified exceptional environmental friendliness, economic feasibility and waste reduction of 63%–93%, reaffirming alignment with sustainability paradigms. These advantages support practical adoption in quality control especially laboratories lacking expensive instrumentation. Overall, the ingenious sensor reconciles nanotechnology innovation with the circular economy ethos to tackle an urgent food safety challenge, guided holistically by sustainability metrics.

Keywords Al_2O_3 -NPs/MWCNTs composite · Eco-sensor · Waste recycling · Food safety · Cyclic voltammetry · Green-and-White analysis

1 Introduction

In today's world, the pursuit of sustainable solutions is more critical than ever, driven by the urgent need to address environmental challenges and preserve our planet's finite

resources. Amidst this backdrop, the concept of the nano-circular economy (NCE) has emerged as a paradigm shift from the traditional linear economic model of "take-make-waste" to a regenerative and holistic approach, where resources are continuously reused and regenerated, leaving no room for waste generation especially materials at the nanoscale [1]. Integrating the principles of the NCE and green and white analytical chemistry (GAC/WAC) into analytical methods promises to contribute to a more sustainable and resource-efficient future that holds great promise for tackling global issues, particularly in the domain of food safety regarding drug residues of zoonotic infection [2, 3].

Schistosomiasis is a widespread helminth zoonotic infection that imposes a significant socioeconomic burden and lacks effective vaccines [4–6]. Praziquantel has long been the treatment of choice; however, emerging risks, including

✉ Sherif M. Eid
sheriefmohammed@o6u.edu.eg; sherief055@icloud.com

¹ Pharmaceutical Analytical Chemistry Department, Faculty of Pharmacy, Al-Azhar University, Nasr City, Cairo 11751, Egypt

² Analytical Chemistry Department, Faculty of Pharmacy, October 6 University, 6 October City, Giza 12585, Egypt

³ Pharmaceutical Analytical Chemistry, School of Pharmacy, Badr University in Cairo, Badr City, Cairo 11829, Egypt

reduced drug susceptibility and resistance, necessitate alternative options [7–9]. Since 2020, cinnarizine (CIN) has shown promise as an antischistosomal agent, demonstrating comparable efficacy to praziquantel, and even surpassing it in the early stages of infection [10, 11]. However, the accumulation of CIN in animal organs and its long withdrawal period of up to 10 days raises concerns about potentially toxic effects on the consumer's central nervous system, leading to conditions such as parkinsonism [12–14]. Furthermore, the long-term ingestion of CIN residues in animal products may pose cardiovascular risks [15, 16]. Therefore, the sensitive detection of CIN residues is paramount for food quality control and consumer safety.

Currently, only one analytical method exists for detecting CIN in food samples, which relies on gas chromatography [17]. This technique is expensive, complex, uses hazardous chemicals, and cannot be utilized for on-site analysis. The scarcity of methods for CIN detection not only highlights the complexity of analysis but also the need for improved detection approaches. Electroanalytical sensors utilizing nanoparticle-modified electrodes have emerged as effective green and white analytical tools due to their sensitivity, selectivity, affordability, minimal solvent usage, stability, reproducibility, and environmentally friendly characteristics [18, 19]. However, existing electroanalytical sensors for CIN detection have complex fabrication, inadequate sensitivity for real samples, and have not been applied to food matrices [20–22]. This work addresses these limitations through square wave voltammetry (SWV) combined with an innovative electrode modification using aluminum oxide nanoparticles (Al_2O_3 -NPs) and multi-walled carbon nanotubes (MWCNTs) on a disposable carbon paste electrode (CPEs). This harnessing of green nanotechnology and circular economy thinking enables an electrochemical sensor for CIN detection utilizing recycled aluminum waste.

SWV technique has gained attention recently for its exceptional ability to analyze faradaic currents and quantify trace substances precisely [23, 24]. CPEs are advantageous owing to their easy modification, low background current, and resistance. However, their detection capabilities are limited [25, 26]. MWCNTs are optimal CPE modifiers, enhancing polymer matrix reinforcement, conductivity, capacitance rates, and stability [27, 28]. Metal oxide nanoparticles augment electrode surface area and charge transfer, enabling ultrasensitive analyte detection [29–31]. Specifically, Al_2O_3 -NPs offer superior affordability, chemical stability over wide pH, availability, and biocompatibility [32].

This first-of-its-kind research harnesses SWV analysis empowered by an Al_2O_3 -NPs/MWCNTs/CP sensor to pioneer major advancements in CIN quantification. Comprehensive characterization validates dramatically enhanced electrochemical properties with remarkable sensitivity surpassing previous sensors by orders of magnitude. The

sensor demonstrates excellent accuracy, precision, stability, reproducibility, and rapid response. Practical applicability for food safety is demonstrated via successful quantification in bovine-derived matrices including liver, milk, kidney, and meat down to nanomolar levels. In addition, the method's exceptional alignment with sustainable practices is evidenced through multidimensional greenness and whiteness assessments using five different tools including, RGB12 (Red Green Blue 12), AGREE (Analytical Greenness Metric), ESA (Eco-Scale Assessment), NEMI (National Environmental Method Index), and ComplexGAPI (Complementary Green Analytical Procedure Index). Collective findings reaffirm minimal waste generation, energy consumption, affordability, and toxicity, cementing the sensor's exceptional alignment with sustainable analytical chemistry principles compared to existing methods. Overall, the ingenious sensor reconciles nanotechnology innovation with the circular economy ethos to tackle an urgent food safety challenge, guided holistically by sustainability metrics.

2 Experimental

2.1 Materials and Reagents

CIN (purity 99.17%) was generously supplied by the Chemical Industries Development Company located in El Haram, Giza, Egypt. Stugerol® tablets, a product of Mina Pharm Pharmaceuticals, Egypt (BN: 805075), were obtained from a local market. These tablets were labeled to contain 25 mg of CIN per tablet. The procurement of ethanol, MWCNTs with a purity greater than 95% (carbon content) and an outer diameter ranging from 6 to 9 nm, with graphite particles (10–20 μm), potassium ferricyanide, hydrochloric acid (36%), sodium carbonate, and paraffin oil was carried out from Sigma-Aldrich. Fresh bovine samples, comprising of kidney, milk, meat, and liver, were procured from a local supermarket in Giza, Egypt. A phosphate buffer (PB) solution was prepared at a concentration of 0.05 M using H_2NaPO_4 and Na_2HPO_4 obtained from the Adwic Egyptian Company. The pH range of the solution was adjusted within the range of 2–6. The buffer solution's pH was attained through the utilization of H_3PO_4 and 0.2 M NaOH.

2.2 Instruments

The PGSTAT101 Potentiostat, manufactured by Metrohm Autolab B.V, Netherlands, was utilized to conduct electrochemical analyses. The electrochemical cell was composed of a working electrode (proposed electrode), a counter electrode (platinum plate), and a reference electrode (Ag/AgCl with KCl 3 mol/L). The pH level of a solution was regulated through the employment of a digital pH meter JENWAY

3510. The process of homogenization of meat, kidney, and liver was carried out using a glass homogenizer manufactured in Korea, model 099ck424.

2.3 Solutions

A 1×10^{-2} M solution of CIN was prepared by dissolving 0.369 g of CIN powder in 50 mL of ethanol, followed by the transfer of the solution to a 100-mL volumetric flask. Subsequently, ethanol (80%) was added to the designated mark, thereby filling the volume. The process of appropriate dilution was conducted to get a fresh working solution of CIN with a concentration of 1×10^{-3} M. The obtained solutions were stored in a darkened glass receptacle at 8°C for a duration of roughly 5 weeks.

2.4 The Process for Fabricating Electrodes

2.4.1 The Synthesis of Al_2O_3 Nanoparticles

A rinsing procedure utilizing water was implemented to cleanse the amassed waste of aluminum foil and eliminate any extrinsic contaminants. The oxide layers were eliminated by subjecting the samples to a 4-h heat treatment in an oven. Subsequently, the pre-treatment of the sample surface was accomplished through a delicate flushing procedure. Subsequently, a quantity of aluminum foil with a mass of 40.0 g was introduced in a solution containing hydrochloric acid (36%) and water in a 1:1 ratio. The mixture was then agitated until the cessation of effervescence, indicating the production of AlCl_3 . Subsequently, the cooling followed by filtration procedures eliminates all residual impurities. The process of precipitating Al_2O_3 involves a gradual addition of 1 M sodium carbonate while ensuring the complete conversion of aluminum chlorides to aluminum oxides. The resulting mixture is then allowed to settle for an hour. Subsequently, the elimination of any precipitated sodium chloride is achieved through the decantation filtration technique and subsequent water washing. The production of aluminum oxide was carried out through a two-step procedure, involving initial filtration of a solution followed by drying for a duration of 3 to 4 h at a temperature of 100°C in an oven. In the end, the gathered specimens undergo a calcination process lasting 5 h at a temperature (500°C) to obtain Al_2O_3 -NPs [32].

2.4.2 Fabricating of Modified and Bare CPEs

The generation of a uniformly mixed paste for fabricating CPE was achieved in a glass mortar by meticulously incorporating 0.3 mL of paraffin oil with 0.4 g of graphite powder. The paste was inserted into the nozzle that was located on the body of the electrode, and the apparatus was electrically

connected through the utilization of Cu wire. The modified CPEs were produced through a meticulous process involving the careful mixing of paraffin oil, graphite powder, MWCNTs (0.3 mL: 0.4 g: 0.08 g), or/and Al_2O_3 -NPs in varying proportions. The mixture was stirred until a uniform paste was obtained. The paste was inserted into the nozzle that was located on the body of the electrode and the apparatus was electrically connected through the utilization of Cu wire.

2.5 The Electrochemical Characterization

The morphology of the proposed nanocomposite was analyzed using transmission electron microscopy (TEM). The proposed nanocomposite's structure was analyzed using a scanning electron microscope (SEM). The identification and analysis of various chemical species present on the surface of the proposed sensor were exhibited using FTIR spectrophotometer. Furthermore, the utilization of the energy-dispersive spectrometer (EDX) played a significant role in illustrating the fundamental constituent elements and surface contamination detection. Providing valuable insights into the structural properties of the electrode materials and identifying the crystalline phases present in the electrode material were demonstrated through the utilization of X-ray diffractometer (XRD) patterns.

We have investigated the voltammetric behavior through the investigation of several parameters such as electrochemical impedance spectroscopy (EIS), cyclic voltammetry (CV), electrode contents, chronoamperometry, Al_2O_3 -NPs percent, scan rate, and pH studies.

2.6 Electrochemical Evaluations

2.6.1 CIN's Electrochemical Behavior as Measured by SWV

Exact quantities of CIN were meticulously introduced and thoroughly incorporated with PB at a pH of 3 within the electrochemical cell. Subsequently, a stream of nitrogen gas was introduced for a duration of 6 min to eliminate any traces of oxygen from the resultant solutions. The study conducted SWV voltammograms at a positive range of potential (0.9 to +1.4 V) using both bare and modified CPEs. The scan rate employed was 0.06 Vs^{-1} .

2.6.2 Calibration Curves Construction

To get the required concentrations, aliquots of CIN working solution were introduced into multiple 50-mL flasks and subsequently mixed thoroughly with PB (pH 3). Subsequently, peak current (I_p) was assessed via SWV. The plotting of the curve for calibration involved the plotting of the concentration (M) against I_p (μA), followed by the computation of CIN regression equations.

2.7 The Method Applications

2.7.1 The Method Application to Kidney, Liver, and Meat Samples

To evaluate the applicability of the developed method to real samples, liver, kidney, and meat samples were selected for analysis. Each sample (5.0 g) was accurately weighed and subjected to fat content removal. Followed by sonication of specimens into reduced proportions and subjected to homogenization utilizing a high-velocity homogenizer operating at 5000 cycle per minute for a duration of 5 min. The homogenates obtained were subsequently stored in a refrigerator at a temperature of 8 °C until the time of analysis.

To prepare the calibration standards, the homogenized samples were blended with 30 mL of ethanol that had been spiked with 0.369 g CIN. The mixture underwent a 15-min sonication process, which was subsequently followed by 15 min of centrifugation at 5000 cycle per minute. The resultant supernatant underwent multiple rounds of extraction and filtration. The filtrate was carried to 100-mL volumetric flasks and subsequently, mixed with ethanol until the mark was reached. This process resulted in the creation of stock standard solutions containing CIN at a concentration of 1×10^{-2} M.

The process of preparing a fresh 1×10^{-3} M CIN working standard solution involved a suitable dilution. The obtained solutions were stored in a darkened glass receptacle in a refrigerator at 8° C for a duration of 5 weeks. To achieve the necessary concentrations of CIN, additional dilution was carried out utilizing PB with a pH of 3. Subsequently, the electrochemical cell was utilized to measure I_p (μ A) via SWV in accordance with the established protocol, and the resultant data were recorded. The plotting of the curve for calibration involved the plotting of the concentration (M) versus I_p (μ A). This facilitated the derivation of CIN regression equations.

2.7.2 The Method Application to Milk Samples

To assess how well the proposed technique fits the analysis of CIN in milk, a Fresh working solution of CIN at 1×10^{-3} M concentration was prepared through appropriate dilution in milk of the stock solution in PB of pH 3. The electrochemical cell was utilized for the measurement of I_p using SWV, following the standardized procedure. The obtained results were meticulously documented. The plotting of the curve for calibration involved the plotting of the concentration (M) versus I_p (μ A), allowing the derivation of regression equations for CIN.

2.7.3 The Method Application to Pharmaceutical Preparation

The Stugeron® tablets, comprising a total of 10 tablets, underwent precise weighing, followed by meticulous pulverization and subsequent combination. A precise amount exactly corresponding to a 1.0×10^{-3} M stock solution was blended with 50 ml ethanol in a volumetric flask with a capacity of 100 ml. Upon undergoing sonication for a duration of 10 min, the solutions underwent filtration. Following that, the volume was increased to 100 ml using the identical solvent. To get the desired concentrations of CIN, a suitable dilution was carried out utilizing PB with a pH of 3. Then, the electrochemical cell was employed to measure the I_p (μ A) through SWV, and the resultant data were recorded. The proposed methodology was employed to quantify the quantity of CIN in a pharmaceutical dosage form. The regression equation provided was utilized to ascertain the concentration of CIN. The computation of percentage recovery, % R, and standard addition methods was employed to ascertain the accuracy of the technique.

3 Results and Discussion

Electroanalytical methods, especially those utilizing nanoparticle-modified electrodes, have emerged as effective tools that satisfy the demands of GAC and WAC due to their user-friendliness, selectivity, sensitivity, affordability, minimal solvent usage, stability, reproducibility, and environmentally friendly characteristics [27, 33]. The SWV technique, renowned for its exceptional ability to discriminate and analyze faradaic currents, sensitivity and quantify trace amounts of substances with greater precision and accuracy, exceptionally square wave voltammograms, and versatility, has gained significant attention recently, particularly for ultrasensitive detection applications [23, 24]. Meanwhile, CPEs are preferred over other carbon-based electrodes because of their ease of modification, minor background current, broad potential range, and minor ohmic resistance. However, limited detection can limit their use [25, 26]. MWCNTs have garnered significant attention as an optimal modifier for CPEs in achieving ultrasensitive detection due to MWCNTs their mechanical reinforcement to the polymer matrix, enhanced conductivity, increased capacitance, faster charge/discharge rates, and enhanced electrochemical stability [27, 28]. In addition, considering the role of nanomaterials in analytical chemistry, various nanomaterials have been extensively employed as modifiers to amplify the efficiency of CPE [25, 28]. Among various types of nanomaterials, metal oxide nanoparticles (MO-NPs) are particularly favored owing to their exceptional capability of augmenting the

active surface area of electrodes. This augmentation leads to enhanced preconcentration of analytes at the electrode, thereby yielding elevated voltammetric performance, increased extraction efficiency, concentrated target analytes from complex sample matrices, remarkably improved detection limits, and enhanced sensitivity [29–31]. Al₂O₃-NPs are currently one of the most popular MO-NPs due to their affordability, superior chemical stability, wide pH range compatibility, availability, cost-effectiveness, and biocompatibility [32]. In addition, the incorporation of Al₂O₃-NPs offers augmentation of the active surface area and expedites the movement of charges, thereby enabling the detection of analytes with unparalleled sensitivity. Consequently, the utilization of the SWV technique, complemented by the Al₂O₃-NPs/MWCNTs/CP sensor

for analysis, is poised to deliver substantial enhancements in analytical performance, thereby achieving outstanding levels of sensitivity.

3.1 Characterization of Electrode Modification

To get insights into the structure and morphology of the suggested electrode modification, widely used imaging microscopy techniques such as SEM and TEM were employed. SEM pictures were recorded at 500 nm magnification to examine the different modifications. The SEM image of Al₂O₃-NPs (Fig. 1) reveals the presence of elongated particles with a spherical shape, exhibiting rough and irregular surfaces. The particles exhibit a cotton-shaped structure with a homogenous distribution, in agreement with previous

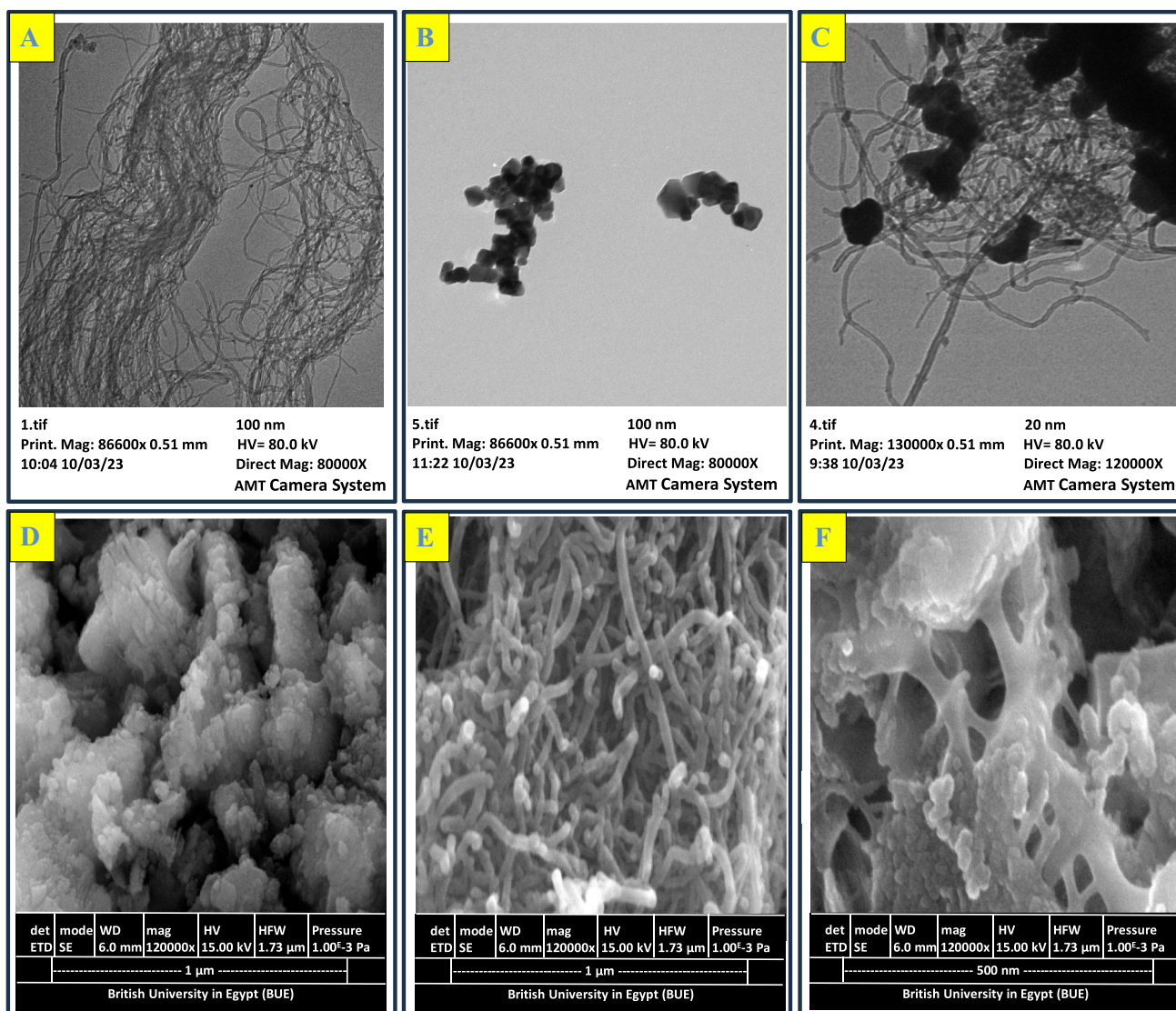


Fig. 1 A TEM picture of MWCNTs, B TEM picture of Al₂O₃-NPs, C TEM picture of Al₂O₃-NPs/MWCNTs, D SEM picture of Al₂O₃-NPs, E SEM picture of MWCNTs, and F SEM picture of Al₂O₃-NPs/MWCNTs

studies [34, 35]. Conversely, the SEM image of MWCNTs displays unique tubes and grooves (Fig. 1). The Al₂O₃-NPs/MWCNTs SEM image (Fig. 1) shows a surface with both tubes and cotton-like structures. This means that there is a good mix of MWCNTs and Al₂O₃-NPs on the surface of the electrode. Based on these SEM images, it can be concluded that the successful incorporation of Al₂O₃ nanoparticles and MWCNTs onto the surface of the CPE resulted in a substantial increase in the effective surface area compared to the unmodified electrode. This modification effectively promotes the movement of charges, thereby facilitating enhanced oxidation reactions and achieving maximum current strength.

In addition, based on the transmission electron microscopy images depicted in Fig. 1, notable alterations in the microstructure of multi-walled carbon nanotubes were observed upon the introduction of Al₂O₃ nanoparticles. This observation provides evidence of the successful integration of semi-spherical Al₂O₃ nanoparticles within the framework of multi-walled carbon nanotubes, which is consistent with the findings from SEM images. Moreover, the TEM analysis revealed that the individual components, Al₂O₃ nanoparticles, multi-walled carbon nanotubes, and Al₂O₃-NPs/MWCNTs composites, exhibited particle sizes ranging between 5 and 10 nm. The relatively narrow particle size distribution of the Al₂O₃-NPs/MWCNTs molecules suggests that the synthesis method used was effective in producing uniform particles.

FTIR spectra of Al₂O₃ nanoparticles and Al₂O₃-NPs/MWCNTs are presented in Fig. 2 to elucidate the various chemical species of the modified electrode. The spectral features of Al₂O₃-NPs, which correspond to the (O–Al–O) bond, are identified within the spectral range of 500–1000 cm⁻¹. The spectral analysis reveals that the MWCNTs possess (-OH) surface functional groups, which are indicated by the 3366–3420 cm⁻¹ wide peak. In addition, the MWCNTs exhibit distinct spectral features related to their carbon framework, particularly the presence of aromatic rings with carbon–carbon double bonds (C=C). This unique property is evident in the prominent peak observed at a wavenumber of 1644.56 cm⁻¹. Based on the FTIR spectra analysis, it can be inferred that the functionalization of MWCNTs and Al₂O₃-NPs onto the surface of CPE has been accomplished effectively, which can enhance the electrocatalytic activity of the modified electrode.

X-ray diffraction analysis was utilized to examine the crystal structure and phase purity of the nanoparticles. The obtained XRD patterns clearly reveal distinct diffraction peaks at specific angles (2θ), indicating the presence of purified Al₂O₃ nanoparticles. Specifically, a prominent diffraction peak was observed at (2θ) = 67.33°, 45.32°, 36.75°, 31.62, and 19.64° corresponding to (440), (400), (311), (220), (111) reflections, respectively (Fig. 2). These peaks

correspond to the 79–1558 standard JCPDS reference code. The X-ray diffraction pattern of the Al₂O₃-NPs/MWCNTs composite exhibits a distinct peak at 26.2°, indicating the successful integration of MWCNTs with Al₂O₃ nanoparticles. Interestingly, the intensity of the diffraction peaks associated with the Al₂O₃-NPs is noticeably diminished in the XRD pattern of the Al₂O₃-NPs/MWCNTs composite. This reduction in intensity can be attributed to the inherent lower-intensity diffraction of MWCNTs in comparison to Al₂O₃-NPs, consistent with previous studies that have reported similar observations [32, 34, 35]. This suggests that the Al₂O₃-NPs are well dispersed within the MWCNTs matrix, indicating a successful integration of the two materials.

The energy-dispersive X-ray spectra obtained for the synthesized Al₂O₃ nanoparticles, MWCNTs, and the composite Al₂O₃-NPs/MWCNTs provide additional evidence confirming the successful synthesis and formation of the modified Al₂O₃-NPs/MWCNTs (Fig. 3). The EDX spectrum of the synthesized Al₂O₃-NPs shows peaks corresponding to aluminum and oxygen, while the EDX of MWCNTs exhibits peaks corresponding to carbon and oxygen. Importantly, the EDX spectrum of Al₂O₃-NPs/MWCNTs confirms the presence of aluminum, carbon, and oxygen, while exhibiting noticeable reductions in carbon and aluminum peaks. These findings strongly support the conclusion that surface modification with Al₂O₃-NPs/MWCNTs has been effectively achieved and the MWCNTs and Al₂O₃-NPs are well attached to the surface of the electrode, indicating successful synthesis of the modified nanoparticles.

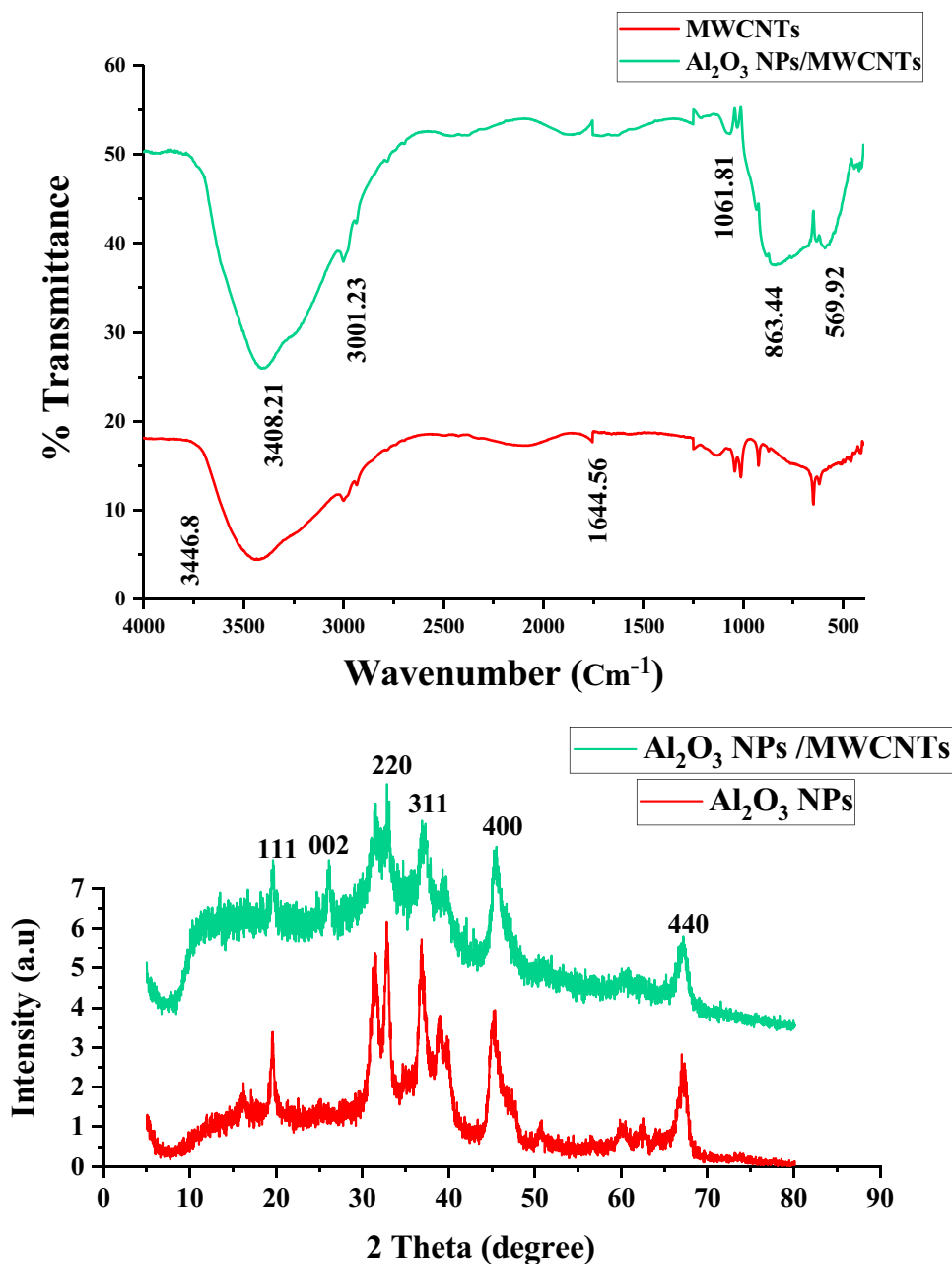
3.2 Electrode Surface Area Determination

The evaluation of the electrochemically effective surface areas for both unmodified and modified CPEs was conducted using the Randles–Ševčík equation [36]:

$$i_{pa} = (D^{1/2} n^{3/2} A v^{1/2} C) 2.69 \times 10^5$$

The equation was applied by analyzing cyclic voltammograms collected from the electrochemical testing of 10⁻³ M of K₃[Fe(CN)₆] in 0.1 M KCl at various scan rates. The calculated electrochemically effective surface area for the bare CPE was determined to be 0.056 cm². Upon modification with MWCNTs, the electrochemically effective surface area of the MWCNTs/CPE composite electrode was found to be 0.164 cm². In addition, the integration of Al₂O₃-NPs with MWCNTs further increased the active surface area, resulting in a measurement of 0.390 cm². Notably, the Al₂O₃-NPs/MWCNTs/CPE composite electrode exhibited a substantially larger electrochemically effective surface area in comparison to its geometric surface area, which was measured to be 0.035 cm². The incorporation of MWCNTs and

Fig. 2 The FTIR, and the XRD of Al_2O_3 nanoparticles and Al_2O_3 -NPs/MWCNTs



Al_2O_3 -NPs in the electrode modification process facilitates the creation of numerous reaction sites, thereby enhancing the catalytic activity and overall efficiency of the electrodes. These findings demonstrate the capability of the modified electrode to provide an amplified electrochemical response, leading to improved sensitivity and detection performance in the analysis of target analytes such as CIN, as shown in Fig. 4.

3.3 Voltammetric Behavior of CIN

To examine the voltammetric characteristics of CIN and the impact of various electrodes on its reaction, CV was

conducted on CIN in PB at a pH of 3 utilizing both unmodified and modified CPEs. The examinations were applied at a positive potential (0.9 to +1.4 V) with a scan rate of 0.06 Vs^{-1} . The obtained voltammograms revealed the presence of an anodic peak (oxidation) at +1.173 V that was irreversible, corresponding to the oxidation of the piperazine ring as it contains an aliphatic tertiary amine that contains lone pair of electrons that can serve as donors. Thus, the oxidation reaction of CIN is most likely centered around the piperazine ring. During the reaction, an electron is donated by nitrogen on the piperazine ring, resulting in the establishment of a positively charged radical, that by gradually eliminating an electron and a proton in a step-by-step manner, a quaternary

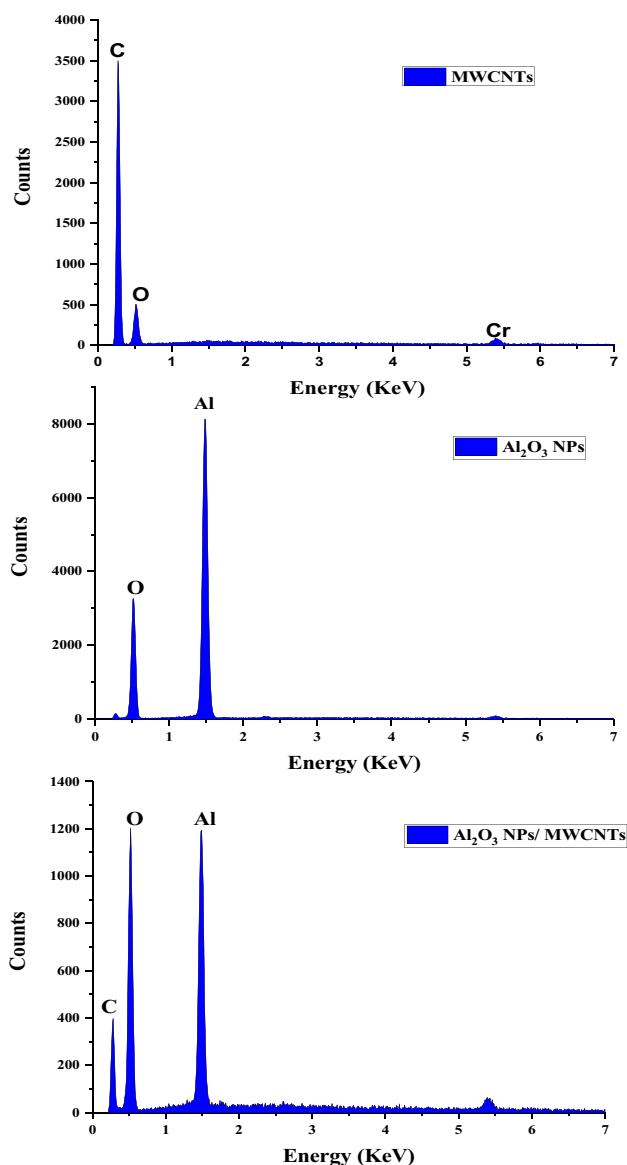


Fig. 3 The EDX spectrum of MWCNTs, Al₂O₃-NPs, Al₂O₃-NPs/MWCNTs

Schiff base is generated. The quaternary Schiff base underwent rapid hydrolysis, yielding the secondary amine, an aldehyde, 3-phenyl-propenal, and 1-benzhydryl-piperazine, as seen in Scheme 1. These observations corroborate the previous findings on the anodic (oxidation) behavior of flunarizine, a fluorinated compound analogous to CIN [37], and the reported findings on the oxidation behavior of CIN [20]. The anodic peak current exhibited a notable increase, rising from 4.81 μ A for the bare electrode to 7.22 μ A for MWCNTs/CPE. Remarkably, when the Al₂O₃-NPs/MWCNTs modifier was employed, the current response further increased to 23.54 μ A, as depicted in Fig. 4. This significant enhancement in the catalytic oxidation of CIN underscores

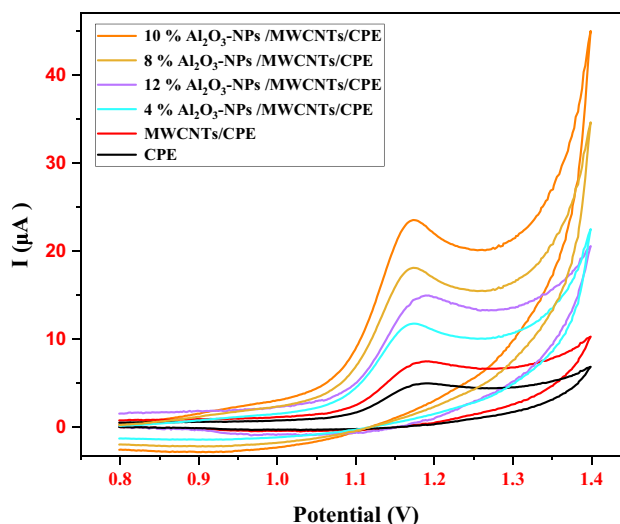


Fig. 4 The different electrodes effect and Al₂O₃-NPs contents on oxidation peak height of CIN using CV

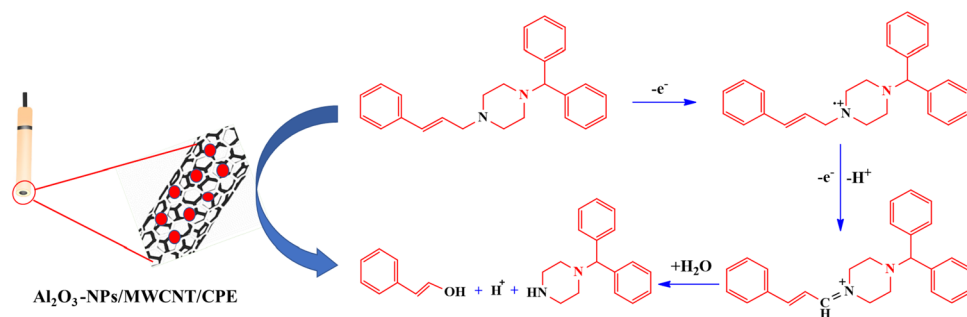
the synergistic effect of the Al₂O₃-NPs/MWCNTs modifiers. The combination of these modifiers demonstrated exceptional efficiency by providing a significant augmentation in the electrochemically effective surface area, a refinement in the flow of electrons, and a boost in the current result. These findings emphasize the high potential of the Al₂O₃-NPs/MWCNTs modifier for enhancing the electrochemical performance of CIN detection. The synergistic effects observed in this study contribute to the advancement of electrochemical sensing platforms, offering improved sensitivity and reliable quantification of CIN in various matrices.

3.4 Maximization of Experimental Parameters

To determine the ideal experimental parameters, we employed CV to investigate several parameters, including the influence of pH, the concentration of Al₂O₃ nanoparticles, deposition potential, the thickness of the electrode, scan rate, kind of buffer, and duration of accumulation. After optimizing the parameters, SWV was utilized to quantify the concentration of CIN.

3.4.1 Influence of Al₂O₃-Nanoparticles Concentrations

The concentration of Al₂O₃-NPs was investigated to determine its influence on the electrochemical performance of the modified electrode. Different concentrations of Al₂O₃-NPs were tested (4, 8, 10, and 12%), and the corresponding CV measurements demonstrated that 10% Al₂O₃-NPs achieved the highest sensitivity and peak current, as shown in Fig. 4.

Scheme 1 Proposed oxidation mechanism of CIN and sensor configuration

3.4.2 Influence of PH

To investigate the influence of pH on the CIN behavior at the 10% $\text{Al}_2\text{O}_3\text{-NPs/MWCNTs/CPE}$ electrode, CV was performed over a pH range of 2 to 6. The results, illustrated in Fig. S1, revealed that a pH of 3 exhibited the highest current intensity, indicating optimal conditions for CIN oxidation. In addition, as the pH increased, a negative shift in the anodic (oxidation) peak potential was noticed, suggesting the involvement of protons in the oxidation reaction of CIN. This observation confirmed the pH dependence of the oxidation process and supported the hypothesis that protons participate in the reaction. The correlation regarding the potential (E_p) and pH was further analyzed, and the equation for regression was obtained, as presented in Fig. S1:

$$E_p(\text{V}) = -0.2973 \text{ pH} + 1.7998$$

The slope of -0.2973, close to 50% of Nernst's theoretical value, which is -0.03 indicated that the CIN oxidation process involves the participation of protons and electrons in a ratio of 1:2. This finding aligns with previous reports on the oxidation behavior of CIN [20] and provides further insight into the mechanistic understanding of the electrochemical oxidation process.

3.4.3 Influence of Scan Rate

To explore the rate-determining mechanism governing the CIN oxidation process at the proposed electrode in question and ascertain whether it is controlled by diffusion or adsorption, CV was recorded at a wide range of scan rates (v) ranging from 0.02–0.14 Vs^{-1} . The obtained results, as depicted in Fig. S2, revealed a positive shift in the oxidation peak potential with elevating scan rate, this suggests that the oxidation reaction of CIN is irreversible in nature. Furthermore, a linear correlation was observed between I_p (μA) and $\log v$ (Fig. S2A). This correlation allowed for the derivation of a regression equation as follows:

$$\log I_p(\mu\text{A}) = 0.5014 \log v + 1.9853$$

The slope, 0.5014, which closely approximates the diffusion-controlled theoretical value of 0.5, provides further evidence supporting the diffusion-controlled kinetic mechanism of CIN. Moreover, the linear correlation between I_p (μA) and $v^{1/2}$ was observed to be linear, as depicted in Fig. S2B. This linear correlation provides further support for the dominant diffusion contribution, as evidenced by the regression equation:

$$I_p(\mu\text{A}) = 96.562v^{1/2} - 0.0581, r^2 = 0.9989$$

To assess the number of electrons involved in the oxidation process (n) at the electrode of interest and the charge transfer constant (k_s), the analysis employed Laviron's equation as follows:

$$E = E^{\circ} + \left(\frac{2.303RT}{anF} \right) \log \left(\frac{RTK^{\circ}}{anF} \right) + \left(\frac{2.303RT}{anF} \right) \log v$$

The determination of the value of (αn) was carried out using the slope of the correlation among $\log v$ and E_p (V), as depicted in Fig. S2C, resulting in a regression equation of

$$E_p(\text{V}) = 0.0578 \log v + 1.2432$$

The calculated slope value of 0.0578 indicated (αn) to be equal to 1.003. Since we treated the CIN reaction as irreversible, we assumed (α) of 0.5. Consequently, the value of (n) was determined to be 2.01 (approximately 2), aligning with the proposed electro-oxidation mechanism of the CIN piperazine ring, as demonstrated in Scheme 1. Furthermore, (k_s) was determined by means of the intercept of the correlation among v and E_p (V), as illustrated in Fig. S2D, resulting in a regression equation of

$$E_p(\text{V}) = 0.3857v + 1.1447$$

The calculated value of k_s was found to be $0.252 \times 10^{-2} \text{ cm s}^{-1}$, which is less than 2×10^{-2} , confirming the irreversibility of the CIN electro-oxidation reaction. Notably, v of 0.06 Vs^{-1} was selected for further analysis and quantification of CIN due to the peak width observed in the data being relatively narrow, indicating a compact and well-defined peak shape.

3.4.4 Chronoamperometry

Four different concentrations of CIN were utilized to evaluate the diffusion coefficient (D) of CIN. The chronoamperograms for four different concentrations of CIN were obtained by maintaining a five seconds-steady potential of 1.173 V in a solution of PB with a pH of 3. The electrode used for this purpose was Al_2O_3 -NPs/MWCNTs/CPE, and the findings are presented in Fig. S3. Subsequently, the value of D was determined through utilization of the Cottrell equation [36], following a series of prescribed procedures: the slopes of the plotted data points were computed with respect to the variable ($t^{-1/2}$). Subsequently, a correlation analysis was performed between the resulting slopes and the corresponding CIN concentrations. The final slope value was found to be equivalent to the (D) of CIN, thus ($D_{\text{CIN}} = 0.413 \times 10^{-4} \text{ cm s}^{-1}$), as depicted in Fig. S3.

3.4.5 Electrochemical Impedance Spectroscopy

EIS plays a vital role in the accurate determination of the electron transfer resistance (R_{ct}) occurring at the surfaces of the electrodes under consideration. The electrodes that were produced underwent electrochemical analysis and impedimetric investigation through the utilization of EIS measurement. A redox probe of 1 mM $\text{K}_4[\text{Fe}(\text{CN})_6]$ was employed, with 0.1 M KCl serving as the supporting electrolyte. The Nyquist plots were obtained as shown, in Fig. 5. The Nyquist plots suggest that the fabricated electrode comprising 10% Al_2O_3 nanoparticles exhibits a reduced semicircle. There is a direct relationship between the dimensions of the semicircle and the (R_{ct}). Consequently, the electrocatalytic properties of 10% Al_2O_3 -NPs/MWCNTs/CPE are superior to those of

MWCNTs/CPE and bare CPE due to their lower (R_{ct}) and enhanced conductivity, as shown in Fig. 5. The resistance values (R_{ct}) were determined by fitting the data, yielding 28.23 $\text{K}\Omega$ for the bare CPE, 9.84 $\text{K}\Omega$ for the MWCNTs/CPE, and 0.83 $\text{K}\Omega$ for the 10% Al_2O_3 -NPs/MWCNTs/CPE composite electrode. The findings agree closely with the cyclic voltammogram outcomes, illustrated in Fig. 4, indicating the cooperative impacts of a composite consisting of 10% Al_2O_3 -NPs/MWCNTs in facilitating the flow of electrons and enhancing the electro-catalysis.

3.5 Validation

The validation procedure was performed following the guidelines set by ICH.

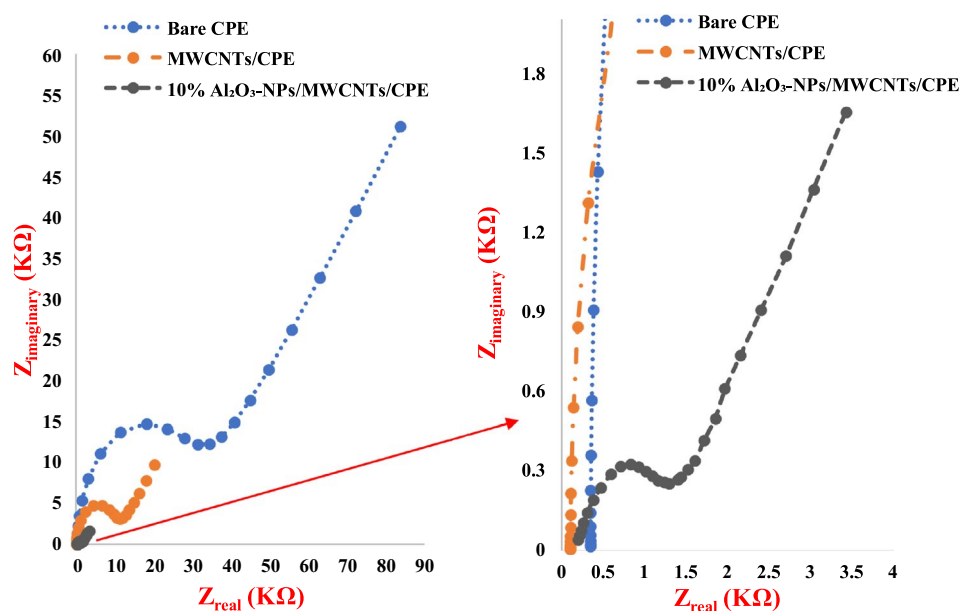
3.5.1 Linearity and Range

The SWV technique was employed to measure the concentration of CIN utilizing the optimized parameters, as depicted in Fig. 6. A linear correlation among the concentrations of CIN and the SWV peak current was observed, indicating satisfactory results. The linear range of CIN was determined to be from 5 to 100 nM, as illustrated in Figure S4. Table 1 displays the regression coefficients.

3.5.2 LOD, and LOQ Limits

The sensitivity of an analytical method is crucial in accurately quantifying target analytes. In this study, the limits of detection (LOD) and quantification (LOQ) were determined to assess the method's sensitivity. The LOD and LOQ were computed employing the equations: $\text{LOD} = 3.3 \sigma/S$ and

Fig. 5 Nyquist plots for modified electrodes (Al_2O_3 -NPs/MWCNTs/CPE and MWCNTs/CPE) and unmodified electrode (CPE)



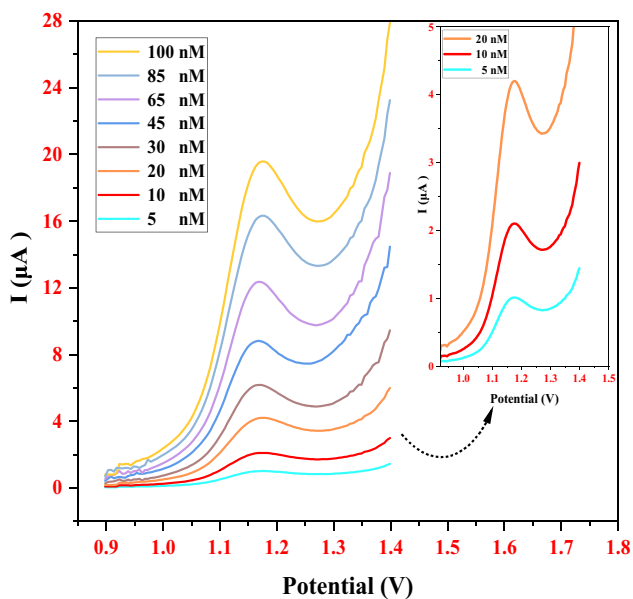


Fig. 6 The SWV of (50–100 nM) of CIN at $\text{Al}_2\text{O}_3\text{-NPs/MWCNTs/CP}$ electrode in phosphate buffer pH 3 at a scan rate of 0.06 Vs^{-1}

Table 1 Validation data of CIN at the $\text{Al}_2\text{O}_3\text{-NPs/MWCNTs/CPE}$

Parameters	CIN
Linearity (nM)	5–100
Intercept	0.2138
Slope	0.1913
Correlation coefficient (r)	0.9995
Accuracy	99.45
Repeatability* (%RSD)	0.59
Intermediate precision** (%RSD)	0.81
Robustness*** (mean \pm %RSD)	99.92 ± 1.3
LOD (nM)	0.17
LOQ (nM)	0.52

* Average of CIN three different concentrations were repeated three times within the day

** Average of CIN three different concentrations were repeated three times in 3 days

*** Variation in method parameters such as pH of the sample and measurement resting period

LOQ = $10 \sigma/S$, as summarized in Table 1. For CIN, the calculated LOD was found to be 0.17 nM, while the LOQ was determined to be 0.52 nM. These values indicate high sensitivity of the presented method, surpassing that reported in the previous study Table 2. The significantly lower LOD and LOQ obtained with our method demonstrate its exceptional ability to detect and quantify CIN at extremely low concentrations. This enhanced sensitivity opens new possibilities for its application in various fields requiring ultrasensitive analysis, such as food quality control and environmental monitoring.

3.5.3 Accuracy

The accuracy of the suggested method was rigorously assessed to ensure reliable and accurate quantification of CIN. The % R, which represents the percentage recovery of CIN, was calculated to assess the method's accuracy. Table 1 presents the obtained % R values with CIN, demonstrating an accurate measurement of 99.45.

3.5.4 Precision

Precision, a crucial parameter for method evaluation, was thoroughly examined to find the repeatability and intermediate precision of the suggested method. Repeatability, also referred to as intra-day precision, and intermediate precision, also known as inter-day precision, were assessed by conducting the evaluation performed on three distinct samples in triplicate on both a single day and across three different days, respectively. The %RSD (relative standard deviation) was determined to quantify precision. The intra-day precision findings yielded a %RSD of ± 0.59 , demonstrating the method's good repeatability within a single day. Similarly, the inter-day precision results showed a %RSD of ± 0.81 , indicating the method's consistency and reproducibility over multiple days. Notably, both %RSD values were below 2%, further affirming the method's high precision and reliability. Table 1 presents a comprehensive summary of the precision assessment, including the %RSD values obtained for both intra-day and inter-day analyses, further supporting the method's suitability for accurate and precise quantification of CIN.

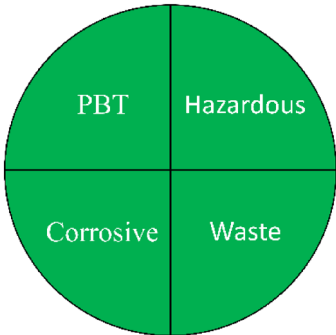
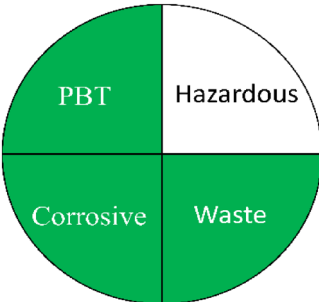
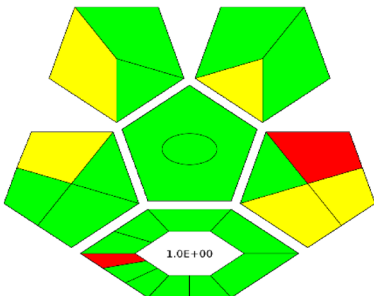
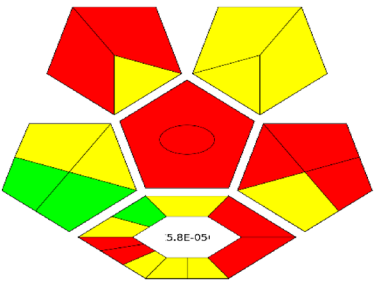

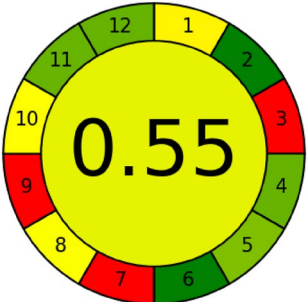
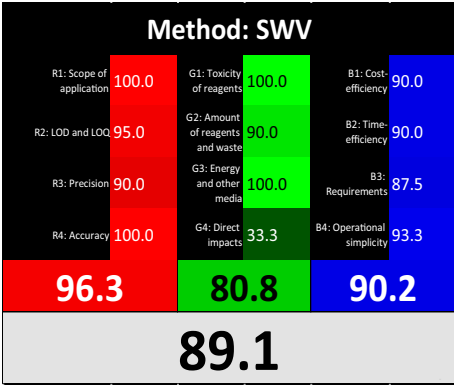
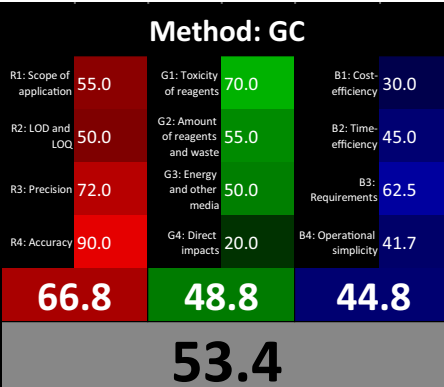
3.5.5 Specificity and Interference Study

To evaluate the specificity of the suggested method, the analysis of CIN in its marketed pharmaceutical preparation was conducted, ensuring the absence of any influence from popular additives. The estimation was performed on Stugeron®, a tablet labeled to contain 25 mg of CIN, as outlined in Table S1. The standard addition technique was employed to validate the procedure's reliability. Triplicate samples with varying concentrations of the standard (10, 20, 30, and 40 nM) were prepared, and the %R of the measured concentration was found as 100.23 ± 1.28 (mean \pm RSD). These findings establish the method's ability to effectively detect and quantify CIN in its intended dose form, with high selectivity and minimal interference from other components, as outlined in Table S1.

3.5.6 Robustness

The robustness of the suggested method, denoting its capacity to maintain consistent performance in the face of slight

Table 2 Comparison of the current method to the proposed method

Parameter	Proposed method	Reported method [17]
Technique used	SWV	GC
Application	Milk, meat, liver, and kidney	Milk
LOD (nM)	0.17	1.36
LOQ (nM)	0.52	4.12
NEMI tool		
ESA Score ^a	85	60
ComplexGAPI tool ^b		
AGREE tool ^c		
RGB 12 ^d algorithm		

^aPenalty points calculation according to the analytical Eco-Scale score (Gałuszka et al., [41])

^bComplexGAPI Assessment evaluated using the Analytical ComplexGAPI Metric approach and Software (Płotka-Wasyłka & Wojnowski, [42])

^cAGREE Assessment evaluated using the Analytical GREENness Metric approach and Software (Pena-Pereira et al., [43])

Table 2 (continued)^dRGB12 whiteness Assessment evaluated using the Analytical RGB 12 algorithm (Nowak et al., [44])

variations in key variables, was thoroughly examined. To assess robustness, two variables, namely the pH value, and scan rate were deliberately altered within a small range (pH value of 3 ± 0.1 , and scan rate value of $0.06 \pm 0.001 \text{ Vs}^{-1}$). The impact of these marginal changes on the analytical outcomes was meticulously investigated, and the results are found in Table 1, providing evidence of the method's robustness.

3.5.7 Reusability, Reproducibility, and Stability

To assess the reproducibility, a series of experiments were conducted using different Al_2O_3 -NPs/MWCNTs/CP electrodes fabricated under identical conditions. The obtained results, as depicted in Fig. S5, revealed consistency among the five electrodes, with a %RSD of ± 0.36 . These findings provide strong evidence for the electrode's high reproducibility. Furthermore, the reusability was evaluated by contrasting the voltammetric readings obtained from an electrode that has been used before with those from an electrode that was only recently manufactured, performed on 10 separate occasions. Remarkably, the two electrodes demonstrated nearly identical responses, indicating that the electrode can be effectively reused without any significant loss in performance. In addition, the stability of the electrode was examined over a period of 4 weeks by consistently monitoring the electrode results employing the suggested method. The obtained responses, illustrated in Fig. S6, demonstrated a favorable level of stability, further supporting the electrode's long-term performance. The combined findings of the reproducibility, reusability, and stability assessments underscore the robustness and reliability of the developed electrode, reinforcing its suitability for practical applications in analytical chemistry and food quality control.

3.6 Application

3.6.1 Veterinary Pharmaceutical Preparation

The application of the developed sensor was successfully demonstrated in the quantification of CIN in veterinary pharmaceutical preparations. The sensor's exceptional performance, combined with its ability to eliminate interference from additives and excipients, underscores its suitability for quality control purposes in the veterinary field, as presented in Table S2. The significant improvement in sensitivity and

detection limit achieved by the proposed method emphasizes its superiority over existing techniques, as shown in Table 2. Furthermore, the successful validation of the SWV applying the standard addition approach further strengthens its credibility and reliability, as shown in Table S1. Overall, the application of the Al_2O_3 -NPs/MWCNTs/CP sensor in veterinary pharmaceutical preparations opens new avenues for efficient and accurate analysis, ensuring the quality and safety of these vital veterinary medications.

3.6.2 Application to Food Samples

To assess the practical applicability of the Al_2O_3 -NPs/MWCNTs/CP sensor, its performance was evaluated in the analysis of various food samples, including milk, liver, kidney, and meat. The developed SWV voltammetric electrochemical method demonstrated exceptional accuracy and precision in the estimation of CIN residues within the concentration range of 5–100 nM, as evidenced by the results presented in Tables S3. The obtained data unequivocally support the reliability and effectiveness of the proposed sensor for the quantification of CIN in milk, kidney, meat, and liver food samples. The sensor exhibited remarkably low detection limits, enabling sensitive detection of CIN without any significant interference. These findings highlight the suitability of the developed sensor as a valuable tool for reliable analysis of CIN residues in diverse food matrices, thus contributing to improved food safety and quality control practices.

4 Greenness/Whiteness Profiles

4.1 Evaluation of the Method's Greenness Profile

In response to the growing demand for analytical processes that prioritize green chemistry considerations, this study places a significant emphasis on evaluating the greenness description of the proposed method. GAC aims to develop cost-effective, automated, and environmentally friendly analytical procedures that minimize sample preparation steps, waste-producing, and the utilization of hazardous chemicals [38, 39]. In alignment with the 12 principles of GAC, various qualitative, semi-quantitative, and quantitative methodologies have recently emerged to assess greenness. To evaluate the greenness of the proposed method, we employed

four widely recognized evaluation tools: AGREE, ESA, NEMI, and ComplexGAPI. These tools enable a comprehensive analysis of different criteria and parameters related to greenness. In Figure S7, the distinctive characteristics and criteria considered by each evaluation tool are clearly depicted, providing a visual representation of their differences. Importantly, a comprehensive evaluation of greenness was conducted to compare the suggested method with the previously published method. By utilizing these evaluation tools, we thoroughly assessed and compared the environmental impact and sustainability of both methods. The results obtained from this evaluation offer valuable insights into the greenness performance of the proposed method, allowing for a comprehensive understanding of its ecological benefits.

4.1.1 Evaluation of the Method's Green Performance Based on NEMI Criteria

In this section, the greenness of the suggested method and the comparison with the published method were evaluated using NEMI, a well-established qualitative tool for assessing greenness [40]. Figure S8 illustrates the four-quadrant circle of NEMI, which is considered green if specific criteria are met. These criteria include: (1) chemicals used in the method not being classified as persistent, bioaccumulative, and toxic (PBT) as per the Environmental Protection Agency's (EPA) and Toxic Release Inventory (TRI) Agency, (2) the chemicals utilized in this procedure are not categorized as hazardous based on the criteria set forth by the (RCRA), specifically in terms of their classification under the U, P, F, D, or TRI lists of potentially hazardous waste, (3) the pH of the method not being corrosive (between 2 and 12), and (4) the quantity of waste produced is below 50 g. For both the reported method and the suggested method, NEMI pictograms were established and are presented in Table 2. Upon comparison, the proposed approach unequivocally surfaced as the most environmentally greenest, as indicated by four green-colored quadrants, satisfying all four NEMI criteria. The chemicals employed in the method were not recognized as hazardous or PBT, the method pH was measured at 3, confirming its non-corrosive nature, and the amount of waste generated was found to be less than 50 g. In contrast, the reported methods exhibited an empty region corresponding to the hazardous category owing to the presence of methanol and heptane-isoamyl alcohol, both categorized as hazardous based on the criteria set forth by the (RCRA), specifically in terms of their classification under the U, P, F, and D.

4.1.2 Evaluation of the Method's Green Performance Based on ESA Criteria

In this section, the environmental sustainability of the suggested method was evaluated by employing a newly proposed semi-quantitative tool, ESA [41]. The ESA assesses the greenness of an analytical methodology by assigning penalty points to handle parameters that are not in accordance with the twelve ideals of GAC, as depicted in Fig. S9. By comparing the ESA scores of the suggested method and the method that was reported, it becomes evident that the suggested method demonstrates superior greenness. The maximum ESA score achieved by the suggested method is 85 points, indicating a high level of adherence to the GAC principles, as summarized in Table 2.

4.1.3 Evaluation of the Method's Performance Based on ComplexGAPI Criteria

In this section, we introduce a thorough evaluation of the greenness of our suggested method utilizing the innovative semi-quantitative tool, ComplexGAPI. This tool has gained significant recognition and acceptance within the chemical society due to its ability to enhance the existing GAPI metric by incorporating a supplementary hexagonal field, based on the CHEM21 parameters. This extended evaluation encompasses all stages of the analytical method, such as sample collection, transportation, preservation, storage, sample preparation, and final analysis [42], as shown in Fig. S10. The ComplexGAPI tool provides an effective means to evaluate and measure the ecological consequences linked to every stage. By employing a color-coded scale, the pictogram generated enables a comprehensive assessment of the degree of greenness at each stage, varying from green to yellow to red. Notably, the ComplexGAPI tool offers shareware software that facilitates the production of ComplexGAPI pictograms, making it user-friendly and accessible. Our presented method demonstrates exceptional greenness, as evidenced by the predominance of green pictograms and the remarkably low E-factor. The E-factor, which stands at an impressive value of one, indicates minimal waste generation, thereby resulting in a positive environmental impact and enhanced sustainability. This highlights the superiority of our proposed method over the method that was reported approach regarding greenness, as summarized in Table 2.

4.1.4 Assessment of Method's Green Performance Based on AGREE Criteria

In this section, we evaluate the greenness of the suggested method in accordance with the widely recognized and

trending greenness evaluation metric, AGREE [43]. AGREE stands out due to its comprehensive nature, encompassing all 12 principles of GAC. It offers flexibility through the option to assign weights to different parameters, provides a clear and easily understandable pictogram as the result, and can be conveniently applied using freely available software. To conduct the assessment, we carefully referenced the 12 crucial ideals of GAC in the entered criteria, allowing for diverse measures to provide a degree of adaptability. The combination of these parameters yields a final score ranging from zero to one. The method's overall level of sustainability can be visually depicted through a clock-like graph, wherein the color and score located at the center signify its overall greenness. A score of one corresponds to dusky green, while a score of zero represents a shade of deep red. Prior to developing inclusive evaluations featuring polychromatic illustrations, we thoroughly documented the essential insights regarding the 12 parameters of GAC for both the suggested method and the method that was reported. The supplementary material provides detailed insights into these assessments. Based on the evaluation using AGREE, the suggested method exhibits outstanding greenness, achieving a high score (0.86), indicating its more efficient performance in terms of green principles. The graphs presented in Table 2 visually demonstrate the greenness of the suggested method, reinforcing its environmentally friendly characteristics and confirming its alignment with sustainable analytical practices.

4.2 Evaluation of the Method's Whiteness Profile

In the assessment of the proposed method's whiteness, the RGB 12 method was introduced as an effective tool for quantitatively evaluating the sustainability level of analytical methods in terms of whiteness assessment [44]. This method comprises 12 distinct algorithms categorized into red, green, and blue groups, each addressing crucial parameters related to sustainability. The green group (G1–G4) focuses on significant parameters such as toxicity, excessive waste and reagent utilization, energy utilization, and the immediate effects on animals, humans, and genetically modified organisms. The group denoted by the color red (R1–R4) assesses validation criteria, encompassing the extent of applicability, the limit of detection, the limit of quantification, precision, and accuracy. The cluster denoted as the blue group, comprising B1 to B4, evaluates the affordability, time-based efficiency, as well as practical and financial prerequisites. By applying the RGB algorithm, the whiteness value, which represents the method's compliance with the ideas of WAC, is estimated by combining the scores obtained for each of the three-color groups. Table 2 illustrates that the suggested approach attains a whiteness value of 88.7 in contrast to the

method that has been reported. The comprehensive evaluation using the RGB 12 algorithm confirms the good performance of the proposed method, highlighting its alignment with sustainability principles and its significant advantages over the existing method. This assessment further emphasizes the method's superior performance, reliability, and economic feasibility, making it a compelling choice for various analytical applications., as depicted in Fig. S11. Overall, this facile sensor demonstrated enhancements across critical analytical criteria including the detection limit, linear response across, stability, reproducibility, response time and applicability in spiked food matrices as shown in Table S4. In addition, five different greenness and whiteness tools quantified exceptional environmental friendliness, economic feasibility and waste reaffirming alignment with sustainability paradigms, as shown in Table 2.

5 Recommendations for Future Work and Limitations

While this study demonstrates the excellent performance of the developed Al_2O_3 -NPs/MWCNTs/CP sensor for the detection of CIN, there remain opportunities to build on this work and address certain limitations. Further research could explore modifying the electrode with other nanomaterials or hybrid composites to potentially enhance sensitivity even beyond what was achieved here. Testing the sensor with a wider range of real food samples, including different types of meat, dairy products, and plant-based foods, would support its broad applicability for food analysis. Regarding limitations, the electrode fabrication procedure requires optimization and standardization for large-scale production. Investigating alternate electrode fabrication methods amenable to mass production could increase adoption. In addition, while selective towards CIN, evaluating selectivity against a comprehensive panel of potential interfering food matrices would further validate performance. Finally, developing integrated, portable devices incorporating the sensor could simplify on-site testing and analysis for practitioners. Connecting the electrode output to smart systems capable of automated data processing and quality control would be tremendously beneficial. Overall, this work successfully demonstrates a proof-of-concept for using sustainable nanocomposite-modified electrodes to address the emerging food safety challenges related to veterinary drug residues. The promising analytical performance shown here establishes a strong foundation to build upon through further enhancements in selectivity, manufacturability, and integration into smart sensing systems. Addressing these limitations can help translate the exceptional lab-based innovation shown into widespread practical implementation.

6 Conclusion

This study presents a novel and highly impactful approach to the detection and quantification of CIN residues in edible food samples employing a cost-effective and eco-friendly electrochemical sensor. The modification of traditional carbon paste electrodes with recycled aluminum oxide nanoparticles and multi-walled carbon nanoparticles significantly enhances the sensitivity and selectivity of the sensor. Comprehensive characterization techniques including TEM, EDX, XRD, FTIR, and SEM confirmed the successful modification process, resulting in an increase in the electrode effective surface area, enabling ultrasensitive analysis with a detection limit of 0.17 nM. This detection limit surpasses this reported in the previous method, highlighting the superior performance of the developed sensor. The assessment of the method's greenness and whiteness using five evaluation tools demonstrates its superiority over the reported method regarding environmental sustainability, analytical performance, and economic feasibility. The suggested method not only meets the rigorous standards of green analytical chemistry but also offers practical solutions for food quality control in low-infrastructure laboratories, where expensive chromatographic devices are often unavailable. Furthermore, the successful utilization of recycled nanoparticles as electrode modifiers sets a precedent for incorporating NCE, green, and white chemistry principles into the electrochemical analysis, fostering the development of sustainable and cost-effective analytical techniques, which advocates for a more sustainable and resilient future in food safety and quality assurance.

Supplementary Information The online version contains supplementary material available at <https://doi.org/10.1007/s13206-024-00144-4>.

Acknowledgements Not applicable.

Funding Open access funding provided by The Science, Technology & Innovation Funding Authority (STDF) in cooperation with The Egyptian Knowledge Bank (EKB).

Availability of Data and Materials All data generated or analyzed during this study are included in this article and its supplementary files.

Declaration

Conflict of interest The authors declare that they have no known competing financial interests or personal relationships that could have appeared to influence the work reported in this paper.

Open Access This article is licensed under a Creative Commons Attribution 4.0 International License, which permits use, sharing, adaptation, distribution and reproduction in any medium or format, as long as you give appropriate credit to the original author(s) and the source, provide a link to the Creative Commons licence, and indicate if changes were made. The images or other third party material in this article are included in the article's Creative Commons licence, unless indicated

otherwise in a credit line to the material. If material is not included in the article's Creative Commons licence and your intended use is not permitted by statutory regulation or exceeds the permitted use, you will need to obtain permission directly from the copyright holder. To view a copy of this licence, visit <http://creativecommons.org/licenses/by/4.0/>.

References

- Gilbertson, L.M., Vikesland, P.J.: Inspiring a nanocircular economy. *Environ. Sci. NANO* **9**, 839–840 (2022). <https://doi.org/10.1039/D2EN90005J>
- Michael, A.M., Lotfy, H.M., Nessim, C.K.: Greenness profile and whiteness assessment of the stability-indicating HPLC method for the assay of levetiracetam. *Microchem. J.* **190**, 108–117 (2023). <https://doi.org/10.1016/j.microc.2023.108669>
- Kelani, K.M., Elzanfaly, E.S., Saad, A.S., Halim, M.K., El-Zeiny, M.B.: Different greenness assessment perspectives for stability-indicating RP-HPLC method used for the assay of isoxsuprine hydrochloride and four nephrotoxic and hepatotoxic photothermal degradation products. *Microchem. J.* **171**, 106–115 (2021). <https://doi.org/10.1016/j.microc.2021.106826>
- McManus, D.P., Dunne, D.W., Sacko, M., Utzinger, J., Vennerwald, B.J., Zhou, X.-N.: Schistosomiasis. *Nat. Rev. Dis. Primers.* **4**, 13–25 (2018). <https://doi.org/10.1038/s41572-018-0013-8>
- Catalano, S., Sène, M., Diouf, N.D., Fall, C.B., Borlase, A., Léger, E., Bâ, K., Webster, J.P.: Rodents as natural hosts of zoonotic schistosoma species and hybrids: an epidemiological and evolutionary perspective from West Africa. *J. Infect. Dis.* (2018). <https://doi.org/10.1093/infdis/jiy029>
- Lai, Y.-S., Biedermann, P., Ekpo, U.F., Garba, A., Mathieu, E., Midzi, N., Mwinzi, P., N'Goran, E.K., Raso, G., Assaré, R.K., Sacko, M., Schur, N., Talla, I., Tchuenté, L.-A.T., Touré, S., Winkler, M.S., Utzinger, J., Vounatsou, P.: Spatial distribution of schistosomiasis and treatment needs in sub-Saharan Africa: a systematic review and geostatistical analysis. *Lancet Infect. Dis.* **15**, 927–940 (2015). [https://doi.org/10.1016/S1473-3099\(15\)00066-3](https://doi.org/10.1016/S1473-3099(15)00066-3)
- Sabra, A.N.A., Botros, S.S.: Response of schistosoma mansoni isolates having different drug sensitivity to praziquantel over several life cycle passages with and without therapeutic pressure. *J. Parasitol.* **94**, 537–541 (2008). <https://doi.org/10.1645/GE-1297.1>
- Mwangi, I.N., Sanchez, M.C., Mkoji, G.M., Agola, L.E., Runo, S.M., Cupit, P.M., Cunningham, C.: Praziquantel sensitivity of Kenyan Schistosoma mansoni isolates and the generation of a laboratory strain with reduced susceptibility to the drug. *Int. J. Parasitol. Drugs Drug Resist.* **4**, 296–300 (2014). <https://doi.org/10.1016/j.ijpddr.2014.09.006>
- Melman, S.D., Steinauer, M.L., Cunningham, C., Kubatko, L.S., Mwangi, I.N., Wynn, N.B., Mutuku, M.W., Karanja, D.M.S., Colley, D.G., Black, C.L., Secor, W.E., Mkoji, G.M., Loker, E.S.: Reduced Susceptibility to Praziquantel among Naturally Occurring Kenyan Isolates of Schistosoma mansoni. *PLoS Negl. Trop. Dis.* **3**, 490–504 (2009). <https://doi.org/10.1371/journal.pntd.0000504>
- Sarhan, R.M., Thabet, H.S., Nazeer, J.T., William, S.: The impact of cinnarizine and griseofulvin on juvenile and adult stages of *Schistosoma mansoni*. *J. Helminthol.* **94**, 29–41 (2020). <https://doi.org/10.1017/S0022149X19000178>
- Xavier, R.P., Mengarda, A.C., Silva, M.P., Roquini, D.B., Salvadori, M.C., Teixeira, F.S., Pinto, P.L., Moraes, T.R., Ferreira, L.L.G., Andricopulo, A.D., de Moraes, J.: H1-antihistamines as antischistosomal drugs: in vitro and in vivo studies.

- Parasit. Vectors **13**, 260–278 (2020). <https://doi.org/10.1186/s13071-020-04140-z>
12. Serrano, A., Menendez, J., Casarejos, M., Solano, R., Gallego, E., Sanchez, M., Mena, M., Garciadeyebenes, J.: Effects of cinnarizine, a calcium antagonist that produces human parkinsonism, in parkin knock out mice. *Neuropharmacology* **49**, 208–219 (2005). <https://doi.org/10.1016/j.neuropharm.2005.03.003>
 13. Teive, H.A.G., Troiano, A.R., Germiniani, F.M.B., Werneck, L.C.: Flunarizine and cinnarizine-induced parkinsonism: a historical and clinical analysis. *Parkinsonism Relat. Disord.* **10**, 243–245 (2004). <https://doi.org/10.1016/j.parkreldis.2003.12.004>
 14. Haress, N.G.: Cinnarizine: comprehensive profile, profiles of drug substances, excipients and related. *Methodology* **40**, 1–41 (2015). <https://doi.org/10.1016/bs.podrm.2015.01.001>
 15. Jhang, K.-M., Huang, J.-Y., Nfor, O.N., Tung, Y.-C., Ku, W.-Y., Lee, C.-T., Liaw, Y.-P.: Extrapyramidal symptoms after exposure to calcium channel blocker-flunarizine or cinnarizine. *Eur. J. Clin. Pharmacol.* **73**, 911–916 (2017). <https://doi.org/10.1007/s00228-017-2247-x>
 16. Kay, J.M., Smith, P., Heath, D., Will, J.A.: Effects of phenobarbitone, cinnarizine, and zoxazolamine on the development of right ventricular hypertrophy and hypertensive pulmonary vascular disease in rats treated with monocrotaline. *Cardiovasc. Res.* **10**, 200–205 (2015). <https://doi.org/10.1093/cvr/10.2.200>
 17. Woestenborghs, R., Michielsens, L., Lorreyne, W., Heykants, J.: Sensitive gas chromatographic method for the determination of cinnarizine and flunarizine in biological samples. *J. Chromatogr. B Biomed. Sci. Appl.* **232**, 85–91 (1982). [https://doi.org/10.1016/S0378-4347\(00\)86010-7](https://doi.org/10.1016/S0378-4347(00)86010-7)
 18. El-sayed, H.M., Abdel-Raouf, A.M., Abdellatef, H.E., Hendawy, H.A.M., El-Abassy, O.M., Ibrahim, H.: Versatile eco-friendly electrochemical sensor based on chromium-doped zinc oxide nanoparticles for determination of safinamide aided by green assessment criteria. *Microchem. J.* **182**, 107–120 (2022). <https://doi.org/10.1016/j.microc.2022.107900>
 19. Atty, S.A., Abdel-raouf, A.M., Fouad, F.A., Mohamed, T.F., Elbardisy, H.M.: Green electrochemical methodology for simultaneous determination of atorvastatin and ezetimibe: Application to biological matrices. *Sustain Chem. Pharm.* **36**, 101–115 (2023). <https://doi.org/10.1016/j.scp.2023.101300>
 20. Hegde, R.N., Hosamani, R.R., Nandibewoor, S.T.: Voltammetric oxidation and determination of cinnarizine at glassy carbon electrode modified with multi-walled carbon nanotubes. *Colloids Surf. B Bioint.* **72**, 259–265 (2009). <https://doi.org/10.1016/j.colsurfb.2009.04.013>
 21. El-Sayed, G.O., Yasin, S.A., El Badawy, A.A.: Voltammetric behavior and determination of cinnarizine in pharmaceutical formulations and serum. *Anal. Lett.* **41**, 3021–3033 (2008). <https://doi.org/10.1080/00032710802463915>
 22. Hegde, R.N., Nandibewoor, S.T.: Voltammetric detection of cinnarizine at multi-walled carbon nanotubes modified carbon paste electrode. *Int. J. Res. Sci. Innov.* **5**, 31–41 (2018). <https://doi.org/10.1016/j.IJRSI.2018.107900>
 23. Arthur, E.G., Ali, H., Hussain, A., O'Neil, G.D.: Square-wave voltammetry enables measurement of light-activated oxidations and reductions on n-type semiconductor/metal junction light-addressable electrochemical sensors. *Anal. Chem.* **6**, 102–120 (2023). <https://doi.org/10.1021/acs.analchem.3c00630>
 24. Sisay, M., Kassa, A., Tesfaye, A.: Highly selective square wave voltammetric determination of gallic acid in groundnut and tea samples using glycine (2-aminoethanoic acid) modified carbon paste electrode. *Sensors Int.* **4**, 205–227 (2023). <https://doi.org/10.1016/j.sintl.2023.100227>
 25. Elgazzar, E., Said, R.A.M., El-Zomrawy, A.A., Ashmawy, A.M., Abdel-Raouf, A.M., Mostafa, W.A., Ibrahim, H., El-Attar, A.-A.M.M.: the fabrication of an innovative extremely sensitive nano green carbon paste electrode amended with the nanocomposite CuO/Y for electrochemical quantification of amprolium in sheep meat and liver samples. *Food Chem.* **385**, 652–668 (2022). <https://doi.org/10.1016/j.foodchem.2022.132668>
 26. State, R.G., van Staden, J.K., State, R.N., Papa, F.: Rapid and sensitive electrochemical determination of tartrazine in commercial food samples using IL/AuTiO₂/GO composite modified carbon paste electrode. *Food Chem.* **385**, 601–616 (2022). <https://doi.org/10.1016/j.foodchem.2022.132616>
 27. Kelani, K.M., Abdel-Raouf, A.M., Ashmawy, A.M., Omran, G.A., Morshedy, S., Wafaa Nassar, A.M., Talaat, W., Elgazzar, E.: Electrochemical determination of dinitolmide in poultry product samples using a highly sensitive Mn₂O₃/MCNTs-NPs carbon paste electrode aided by greenness assessment tools. *Food Chem.* **382**, 691–702 (2022). <https://doi.org/10.1016/j.foodchem.2021.131702>
 28. Li, G., Feng, S., Yan, L., Yang, L., Huo, B., Wang, L., Luo, S., Yang, D.: Direct electrochemical detection of Cu(II) ions in juice and tea beverage samples using MWCNTs-BMIMPF₆-Nafion modified GCE electrodes. *Food Chem.* **404**, 134–149 (2023). <https://doi.org/10.1016/j.foodchem.2022.134609>
 29. Ghanavati, M., Tadayon, F., Basiryamahabadi, A., Torabi Fard, N., Smiley, E.: Design of new sensing layer based on ZnO/NiO/Fe₃O₄/MWCNTs nanocomposite for simultaneous electrochemical determination of Naproxen and Sumatriptan. *J. Pharm. Biomed. Anal.* **223**, 115–91 (2023). <https://doi.org/10.1016/j.jpba.2022.115091>
 30. Ali, A.-M.B.H., Rageh, A.H., Abdel-aal, F.A.M., Mohamed, A.-M.I.: Anatase titanium oxide nanoparticles and multi-walled carbon nanotubes-modified carbon paste electrode for simultaneous determination of avanafil and doxorubicin in plasma samples. *Microchem. J.* **185**, 250–261 (2023). <https://doi.org/10.1016/j.microc.2022.108261>
 31. Gloria, E., Uwaya, K.B.: Integration of multiwalled carbon nanotubes with cobalt oxide for smart electrochemical sensing of epicatechin in foods. *Carbon Trends.* **10**, 228–240 (2023). <https://doi.org/10.1016/j.cartre.2022.100240>
 32. Nduni, M.N., Osano, A.M., Chaka, B.: Synthesis and characterization of aluminium oxide nanoparticles from waste aluminium foil and potential application in aluminium-ion cell. *Clean Eng. Technol.* **3**, 1–9 (2021). <https://doi.org/10.1016/j.clet.2021.100108>
 33. Somashekarappa, K.K., Halappa, R.B., Rajendrachari, S.: Green chemistry applications in electrochemical sensors. *Recent Dev. Green Electrochem. Sensors.* **1437**, 23–37 (2023). <https://doi.org/10.1021/bk-2023-1437.ch002>
 34. Jbara, A.S., Othaman, Z., Ati, A.A., Saeed, M.A.: Characterization of γ -Al₂O₃ nanopowders synthesized by co-precipitation method. *Mater. Chem. Phys.* **188**, 24–29 (2017). <https://doi.org/10.1016/j.matchemphys.2016.12.015>
 35. Nila, A.S.S.: Synthesis and XRD, FTIR studies of alumina nanoparticle using Co-precipitation method. *Int. J. Res. Appl. Sci. Eng. Technol.* **6**, 2493–2496 (2018). <https://doi.org/10.22214/ijraset.2018.3402>
 36. Attia, K.A.M., Abdel-Raouf, A.M., Serag, A., Eid, S.M., Abbas, A.E.: Innovative electrochemical electrode modified with Al₂O₃ nanoparticle decorated MWCNTs for ultra-trace determination of tamsulosin and solifenacin in human plasma and urine samples and their pharmacological dosage form. *RSC Adv.* **12**, 17536–17549 (2022). <https://doi.org/10.1039/d2ra01962k>

37. Uslu, B., Yılmaz, N., Erk, N., Özkan, S.A., Şentürk, Z., Biryol, I.: The study of the voltammetric behaviour of flunarizine. *J. Pharm. Biomed. Anal.* **21**, 215–220 (1999). [https://doi.org/10.1016/S0731-7085\(99\)00096-5](https://doi.org/10.1016/S0731-7085(99)00096-5)
38. Mahmoud, S.A., Abbas, A.E.F., Katamesh, N.S.: Greenness, whiteness, and blueness assessment with spider chart solvents evaluation of HPTLC-densitometric method for quantifying a triple combination anti-*Helicobacter pylori* therapy. *Sustain Chem. Pharm.* **37**, 401–412 (2024). <https://doi.org/10.1016/j.scp.2023.101412>
39. Attia, K.A.M., El-Olemy, A., Serag, A., Abbas, A.E.F., Eid, S.M.: Environmentally sustainable DRS-FTIR probe assisted by chemometric tools for quality control analysis of cinnarizine and piracetam having diverged concentration ranges: Validation, greenness, and whiteness studies. *Spectrochim. Acta. A Mol. Biomol. Spectrosc.* **302**, 1–15 (2023). <https://doi.org/10.1016/j.saa.2023.123161>
40. Keith, L.H., Gron, L.U., Young, J.L.: Green analytical methodologies. *Chem. Rev.* **107**, 2695–2708 (2007). <https://doi.org/10.1021/cr068359e>
41. Gałuszka, A., Migaszewski, Z.M., Konieczka, P., Namieśnik, J.: Analytical Eco-Scale for assessing the greenness of analytical procedures. *TrAC Trends Anal. Chem.* **37**, 61–72 (2012). <https://doi.org/10.1016/j.trac.2012.03.013>
42. Płotka-Wasyłka, J., Wojnowski, W.: Complementary green analytical procedure index (ComplexGAPI) and software. *Green Chem.* **23**, 8657–8665 (2021). <https://doi.org/10.1039/d1gc02318g>
43. Pena-Pereira, F., Wojnowski, W., Tobiszewski, M.: AGREE—analytical GREENness metric approach and software. *Anal. Chem.* **92**, 10076–10082 (2020). <https://doi.org/10.1021/acs.analchem.0c01887>
44. Nowak, P.M., Wietecha-Posłuszny, R., Pawliszyn, J.: White analytical chemistry: an approach to reconcile the principles of green analytical chemistry and functionality. *TrAC Trends Anal. Chem.* **138**, 1–12 (2021). <https://doi.org/10.1016/j.trac.2021.116223>

Publisher's Note Springer Nature remains neutral with regard to jurisdictional claims in published maps and institutional affiliations.